

## An Analysis of Impedance in the Kolbe Reaction on Platinum and Gold Anodes in Aqueous Acetate Solutions

Isao SEKINE\* and Hideki OHKAWA

Department of Industrial Chemistry, Faculty of Science and Technology,  
Science University of Tokyo, Noda, Chiba 278

(Received July 31, 1978)

The Kolbe reaction occurring on platinum or gold anodes in aqueous acetate was studied by analyzing the equivalent circuit of the impedance obtained with a phase-sensitive detector. In the case of platinum, the equivalent circuit at the potential for the Kolbe reaction is represented by a parallel combination of the double-layer capacity,  $C_{dl}$ , and the charge-transfer resistance,  $\theta$ , in series with the solution resistance,  $R_{sol}$ . The  $C_{dl}$  value of 2.00 V obtained by a complex impedance plane plot is nearly identical to that calculated by assuming that the Helmholtz layer is occupied by  $\text{CH}_3\text{COO}^-$ . In the potential range more negative than 2.00 V, the Kolbe reaction occurs. The steep decrease in the differential capacity is considered to be a result of the decrease in the adsorption pseudo-capacity. The  $\theta$  value of the oxygen evolution increases with an increase in the acetate concentrations. It is shown that the surface coverage of  $\text{CH}_3\text{COO}^-$  may be obtained by "Frumkin's treatment" in conjunction with the high-frequency capacitance,  $C_{HF}$ , and the low-frequency capacitance,  $C_{LF}$ , from the complex capacitance plane plot ( $Y/\omega$  plane plot). The Kolbe reaction does not occur at all with gold anodes, and the specific circular arc was not seen in the  $Y/\omega$  plane plot. Impedance measurements, therefore, confirm that an adsorption pseudo-capacity of  $\text{CH}_3\text{COO}^-$  is not present with gold anodes.

Electrochemical studies of the Kolbe reaction using various techniques have been reported by many investigators.<sup>1-3</sup> The Kolbe reaction was, for example, examined with platinum or gold anodes in acetate or propionate solutions.<sup>4-7</sup> In aqueous acetate solutions the Kolbe reaction proceeds efficiently on platinum at anodic potentials greater than *ca.* 2.00 V, with the release of ethane and carbon dioxide, whereas the reaction does not occur at any potentials on gold anodes.<sup>1</sup> These phenomena result from the difference in anode surface states; ellipsometry<sup>8</sup> shows that the adsorption of a layer of  $\text{CH}_3\text{COO}^-$  or  $\text{CH}_3\text{COO}\cdot$  about 10 Å thick on the platinum at anodic potentials greater than 2.00 V is favorable to the Kolbe reaction, while the oxide ( $\text{Au}_2\text{O}_3$ ) more than 30 Å thick formed on gold anodes inhibits the reaction.

According to an analysis of the impedance of the Kolbe reaction by Kunugi *et al.*,<sup>9</sup> the double-layer capacity decreases from 30 to 10  $\mu\text{F}/\text{cm}^2$  when the anodic reaction changes from the oxygen evolution to the Kolbe reaction. Such behavior can be explained by attributing it to the change from the acetate ion to the methyl radical. However, only this explanation for these phenomena seems not to be sufficient. Furthermore, the equivalent circuit has not appeared in the literature.

In the present study, impedance measurements were made on platinum and gold anodes in aqueous acetate solutions using a phase-sensitive detector (PSD). The equivalent circuits corresponding to the adsorbed layer on the platinum anode or the oxide layer on the gold anode are derived from the impedance analysis. The possibility of the occurrence of the Kolbe reaction is discussed.

### Experimental

**Apparatus.** The impedance was measured with a PSD (Fuso Seisakusho, model 332). The reference signal of the sinusoidal wave in PSD was within 3.5 mV (RMS) over the frequency range of 9 kHz—10 Hz.

**Electrodes.** A section (0.10 cm in diameter) of platinum or gold wire served as the working electrode. The pretreatment of these anodes was carried out as has been described previously.<sup>4</sup> The counter electrode was a spiral platinum wire. The potential was measured with reference to a saturated calomel electrode (SCE), and the electrode was gradually polarized to the positive potential with 10 mV/s. The parallel capacity and resistance were simultaneously plotted with a two-pen recorder. All the circuits were shielded and grounded.

**Solutions.** Test solutions were prepared from the reagent-grade chemicals and triply distilled water. Acetic acid was refluxed in the presence of potassium permanganate to oxidize the contaminating aldehydes, and was then redistilled in the presence of fresh diphosphorus pentaoxide to remove the water. Potassium acetate was used without further purification. The aqueous acetate solutions used were 1:1 mixtures of equimolar solutions of potassium acetate and acetic acid at 0.5, 1, 2, and 5 M respectively. All the experiments were carried out at 25 °C.

### Results and Discussion

**Platinum Electrode.** It has previously been reported that the remarkable decrease at 2.00 V in the differential capacity obtained by an impedance bridge is a necessary condition to promote the Kolbe reaction on a platinum anode in an aqueous acetate solution.<sup>4</sup>

Figure 1 shows the relationship between the parallel capacitance and the potential ( $C_p - E$ ), as measured by a PSD. Two peaks were observed at around 0.80 and 1.35 V. The capacity at potentials greater than 1.35 V markedly decreases and levels off to a constant value at 2.25 V. It has already been reported that an oxygen evolution reaction and adsorption of  $\text{CH}_3\text{COO}^-$  compete in the potential range where the Kolbe reaction does not occur. Such a competition can be analyzed with the aid of the complex impedance plane plot<sup>10</sup> ( $Z$  plane plot) obtained at various acetate concentrations.

Figure 2 shows the results of the  $Z$  plane plot observed on a platinum anode at various acetate concentrations.

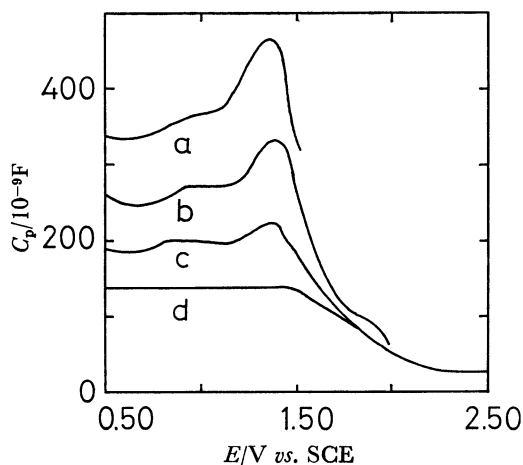


Fig. 1. Parallel capacitance *vs.* potential curves on Pt in 2 M acetate with various frequencies. sweep rate: 10 mV/s, a: 15 Hz, b: 60 Hz, c: 3 kHz, d: 8 kHz.

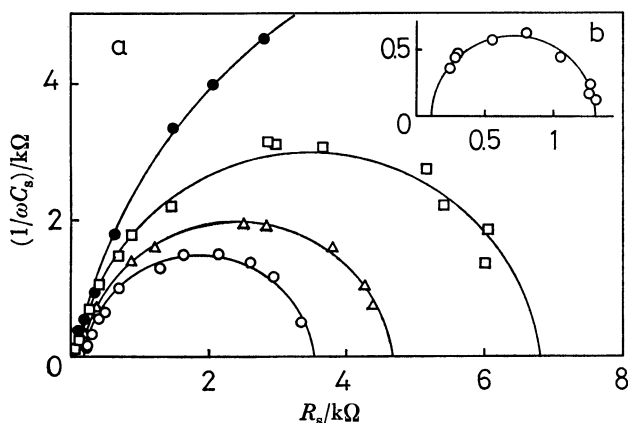


Fig. 2. Complex impedance plane plot of Pt in various acetate concentrations. a: 1.50 V,  $\circ$ —: 0.5 M,  $\triangle$ —: 1 M,  $\square$ —: 2 M,  $\bullet$ —: 5 M, b: 2.00 V,  $\circ$ —: 0.5 M.

The diameter of the semicircle in the Z plane shows the charge-transfer resistance,  $\theta$ . If the value of  $\theta$  at 1.50 V is determined only by oxygen evolution, it will not be affected by the acetate concentrations. Since  $\theta$  increases with an increase in the acetate concentration, it may be concluded that an oxygen-evolution reaction is inhibited by the adsorption of  $\text{CH}_3\text{COO}^-$ . Since the loci of the Z plane plot are given only by the semicircle, the rate-determining step of the Kolbe reaction or the oxygen evolution on the platinum is regarded as a charge-transfer process, representing an activation polarization.

The  $C_{dl}$  values at each concentration, as calculated from,  $\omega_{\max}(=1/\theta C_{dl})$ , corresponding to the top of the semicircle, are shown in Fig. 3. At more negative potentials than 2.00 V, where the oxygen evolution proceeds, the  $C_{dl}$  value of platinum depends on the bulk concentration of the acetate ion and decreases with an increase in the concentration. By contrast,  $C_{dl}$  at 2.10 V, where the Kolbe reaction proceeds, is almost independent of the bulk concentration. From the above results, it can be said that, when the electrode

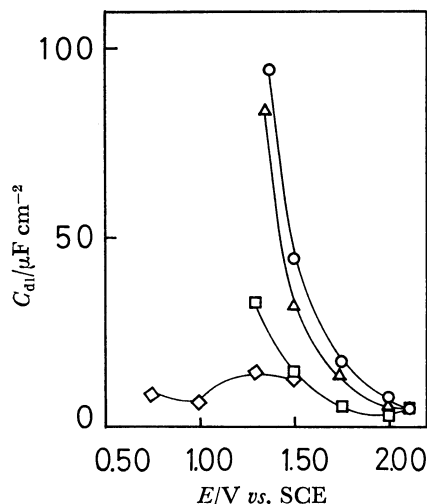


Fig. 3. Double layer capacity *vs.* potential plots.  $\circ$ —: Pt-0.5 M,  $\triangle$ —: Pt-2 M,  $\square$ —: Pt-5 M,  $\diamond$ —: Au-5 M.

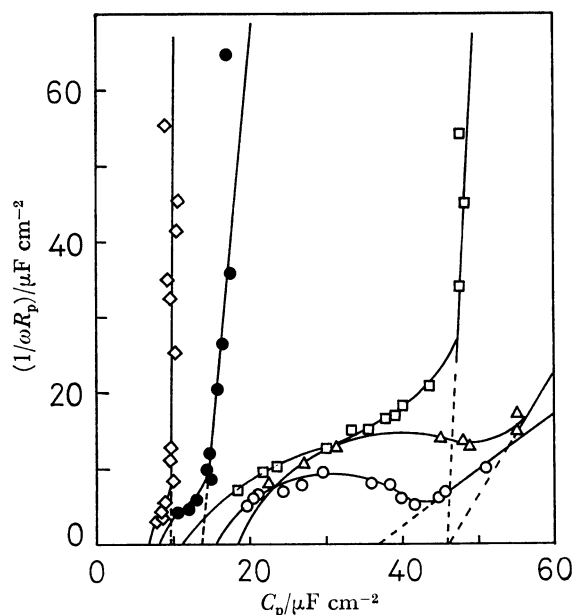


Fig. 4. Complex capacitance plane plot of Pt in 0.5 M acetate.  $\circ$ —: 0.75 V,  $\triangle$ —: 1.37<sub>5</sub> V,  $\square$ —: 1.50 V,  $\bullet$ —: 1.75 V,  $\diamond$ —: 2.00 V.

reaction changes from the oxygen evolution to the Kolbe reaction,  $C_{dl}$  decreases and then remains approximately constant ( $5\text{--}8\ \mu\text{F}/\text{cm}^2$ ). Such behavior in  $C_{dl}$  was found to be similar to that observed for  $C_p$  in the  $C_p$ — $E$  curve described above.

To elucidate further the decrease and then the constancy in  $C_{dl}$  at the potential where the Kolbe reaction proceeds, the above results were analyzed on the basis of the complex capacitance-plane plot<sup>11,12)</sup> ( $Y/\omega$  plane plot) (Fig. 4). At the more negative potentials than 2.00 V, the quarter circle was found in the high-frequency region, while the straight line was found in the lower-frequency region.

If the high-frequency capacitance,  $C_{HF}$ , is determined by extrapolation to an infinite frequency ( $\omega=\infty$ ) in a

quarter circle, and the low-frequency capacitance,  $C_{LF}$ , by linear extrapolation to the  $C_p$  axis, the definitions of  $C_{HF}$ ,  $C_{LF}$  and the adsorption pseudo-capacity,  $\Delta C$ , are as follows:<sup>13)</sup>

$$C_{HF} = (\partial q / \partial E)_{\mu, \Gamma} \quad (1)$$

$$C_{LF} = (\partial q / \partial E)_{\mu} = (\partial q / \partial E)_{\mu, \Gamma} + (\partial q / \partial \Gamma)_{\mu, E} (\partial \Gamma / \partial E)_{\mu} \quad (2)$$

$$\Delta C = C_{LF} - C_{HF} = (\partial q / \partial \Gamma)_{\mu, E} (\partial \Gamma / \partial E)_{\mu} \quad (3)$$

where  $\Gamma$ ,  $q$ , and  $\mu$  represent surface excess, the surface charge density, and the chemical potential respectively.

The quarter circle was obtained at 0.75 and 1.35 V, where the first and second capacity peaks were obtained respectively in the  $C_p$ - $E$  curves. It is known that the first capacity peak is due to an adsorption of oxygen-containing species ( $\text{OH}^-$ ,  $\text{H}_2\text{O}$ ,  $\text{O}^{2-}$ , etc.)<sup>4)</sup> and that the rate-determining step of adsorption is a diffusion process when the  $Y/\omega$  plane plot gives a quarter circle.<sup>11,12)</sup> As has been described above, the adsorption of oxygen-containing species is diffusion-controlled and the adsorption pseudo-capacity gives a value of 10–20  $\mu\text{F}/\text{cm}^2$ . The second peak is regarded as the adsorption of  $\text{CH}_3\text{COO}^-$  in the potential range of oxygen evolution.<sup>4)</sup> In this case, the  $\text{CH}_3\text{COO}^-$  is specifically adsorbed by forming a partly covalent bond with platinum and is perhaps responsible for the pseudo-capacity.<sup>14)</sup>

Since the  $Y/\omega$  plane plot gives a quarter circle at 1.37<sub>5</sub> V, the rate-determining step in the adsorption of  $\text{CH}_3\text{COO}^-$  is a diffusion-controlled process and produces an adsorption pseudo-capacity,  $\Delta C$ . A  $\Delta C$  value of 20  $\mu\text{F}/\text{cm}^2$  is observed at 1.37<sub>5</sub> V. In the  $C_p$ - $E$  curve noted above, the  $C_p$  value decreased markedly with an increase in the positive potentials to more than 1.30–1.40 V indicated a second capacity peak, and  $C_{dl}$  decreased similarly (Figs. 1 and 3). These results can be explained by a diminution of the quarter circle, representing the magnitude of the adsorption pseudo-capacity,  $\Delta C$ ; i.e., if  $(\partial \Gamma / \partial E)_{\mu} = 0$  in Eq. 3, the  $\Delta C$  due to the adsorption of  $\text{CH}_3\text{COO}^-$  will vanish. The above conditions are satisfied by the fact that  $\Gamma$  for the adsorption of  $\text{CH}_3\text{COO}^-$  is constant against the potentials. The limiting case in the  $Y/\omega$  plane plot is at 2.00 V, where the quarter circle almost disappears and a straight line is obtained.

In order to determine the surface coverage of  $\text{CH}_3\text{COO}^-$  from the  $C_{HF}$  values, "Frumkin's treatment" was performed. If the electric double layer is constructed by two parallel condensers, one is covered by the adsorbate, while the other is not; the charge on the electrodes is then given as follows:<sup>15)</sup>

$$q = q_0(1 - \theta_s) + q^*\theta_s$$

where  $q_0$  and  $q^*$  correspond to the electrode charges when  $\theta_s = 0$  and  $\theta_s = 1$  respectively; and where  $\theta_s$  is the fractional coverage of the surface ( $= \Gamma / \Gamma_{\text{max}}$ ). The  $C_{LF}$  value given in Eq. 2 is converted to Eq. 4:

$$C_{LF} = dq/dE = (\partial q / \partial E)_{\theta_s} + (\partial q / \partial \theta_s)(d\theta_s/dE) = \{C_0(1 - \theta_s) + C^*\theta_s\} + (q^* - q_0)(d\theta_s/dE) \quad (4)$$

where  $C_0 = dq_0/dE$  and  $C^* = dq^*/dE$ . The first two terms of Eq. 4 are replaced by Eq. 1 and:

$$C_{HF} = (\partial q / \partial E)_{\theta_s} = C_0(1 - \theta_s) + C^*\theta_s \quad (5)$$

As an example,  $\theta_s$  of  $\text{CH}_3\text{COO}^-$  was obtained from the platinum anode in a 2 M acetate solution; the values of  $C_{HF}$  for  $C^*$  and  $C_0$  were 6 and 24  $\mu\text{F}/\text{cm}^2$ , obtained at 2.00 and 0.90 V, respectively. Because the adsorption of  $\text{CH}_3\text{COO}^-$  is negligible at potentials less than 1.30 V, as shown by a previous study,<sup>9)</sup> the condition of  $\Delta C \approx 0$  is satisfied at 2.00 V in Fig. 4. The values of  $\theta_s$  were calculated from Eq. 5; e.g., when  $C_{HF} = 20 \mu\text{F}/\text{cm}^2$  at 1.50 V, then  $\theta_s = 0.2$ , and when  $C_{HF} = 12 \mu\text{F}/\text{cm}^2$  at 1.75 V,  $\theta_s = 0.7$ . The  $\theta_s$  values obtained by the above method agreed approximately with the surface coverage obtained from the difference between the currents observed in the presence and in the absence of acetate ions in a phosphate solution using the linear-potential-sweep method.

The admittance for a first-order electrode reaction proceeding on the  $Y/\omega$  plane is characterized by Eq. 6.<sup>16)</sup> Since only the perpendicular line against the  $C_p$  axis is observed, the straight lines obtained at 1.50 and 1.75 V indicate that the oxygen evolution follows a first-order electrode reaction:

$$Y/\omega = jC_{dl} + 1/\omega\theta \quad (6)$$

The intercept at the  $C_p$  axis gives both  $C_{dl}$  and  $C_{LF}$ , according to Eq. 6. Therefore, it may be concluded that the  $C_{dl}$  value on the  $Z$  plane at the potentials of oxygen evolution contains the adsorption pseudo-capacity,  $\Delta C$ , of  $\text{CH}_3\text{COO}^-$ . For example, at 1.50 V in a 2 M acetate solution, the  $C_{dl}$  obtained on the  $Z$  plane corresponding to  $C_{LF}$  on the  $Y/\omega$  plane is 33  $\mu\text{F}/\text{cm}^2$ . Consequently,  $\Delta C (= C_{LF} - C_{HF})$  is 13  $\mu\text{F}/\text{cm}^2$ , since  $C_{HF}$  is equal to 20  $\mu\text{F}/\text{cm}^2$ . For the above derivation, the adsorption of  $\text{CH}_3\text{COO}^-$  was taken to proceed simultaneously with the oxygen evolution on the  $Y/\omega$  plane.

As  $\Delta C$  approximates zero at 2.00 V, where the Kolbe reaction proceeds, the  $C_{dl}$  value extrapolated to the  $C_p$  axis almost represents that of  $C_{HF}$ . Thus, a  $C_{HF}$  value of 5–6  $\mu\text{F}/\text{cm}^2$  was found at 2.00 V in 0.5–2 M acetate solutions. Accordingly, the equivalent circuit of platinum at potentials less than 2.00 V is shown in Fig. 5(a). That the adsorption of  $\text{CH}_3\text{COO}^-$  is the diffusion-controlled process and gives the pseudo-capacity,  $\Delta C$ , is shown by the elements of  $C_{HF}$ ,  $\Delta C$ , and  $Z_w$ . This impedance,  $Z_w$ , is considered to be equivalent to the Warburg impedance in a diffusion process:

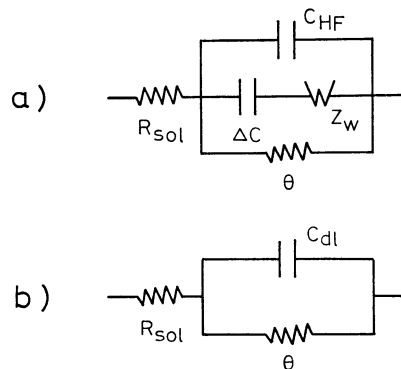


Fig. 5. Electrical equivalent circuit.

$$Z_w = (1-j)(\tau_D/2\omega)^{1/2} \cdot \Delta C^{-1} \quad (7)$$

$$\tau_D = (\partial F / \partial C_A)_E^2 / D$$

$\tau_D$ : mean diffusion-controlled relaxation time;

$C_A$ : concn of adsorbate;  $D$ : diffusion coefficient.

The coefficient,  $(\tau_D/2)^{1/2} \cdot \Delta C^{-1}$ , was about 200–400  $\Omega \cdot \text{cm}^2 \cdot \text{s}^{-1/2}$  in the potential range from 0.90 to 1.50 V in the 0.5 M acetate solution. The  $\tau_D$  was calculated from  $\omega_{\max} (=1/\tau_D)$ , corresponding to the top of the quarter circle. The  $\theta$ , combined with other parallel elements, shows the charge-transfer resistance for the oxygen-evolution reaction. Since  $\Delta C$  is almost equal to zero at potentials greater than 2.00 V, the equivalent circuit for the Kolbe reaction is simply shown by Fig. 5(b).

The facts that  $C_p$  is constant at potentials greater than 2.00 V and that  $C_{dl}$  decreases to an almost constant value of 5–8  $\mu\text{F}/\text{cm}^2$  result from the fact that: the constancy in  $C_{dl}$  is explained on the basis of the concept of electric double layer, and the results of ellipsometry.<sup>8)</sup> The total capacitance,  $C_{dl}$ , is generally considered to be the serial combination of a Helmholtz capacity,  $C_H$ ; a diffuse double-layer capacity,  $C_D$ , and a film capacity,  $C_{film}$ , due to the formation of a film on a solid electrode interface:

$$1/C_{dl} = 1/C_{film} + 1/C_H + 1/C_D \quad (8)$$

Since a sufficiently high concentration is employed in this study  $1/C_D$  becomes small and:

$$1/C_{dl} = 1/C_{film} + 1/C_H \quad (9)$$

According to Hoare,<sup>17)</sup> oxygen evolves from the platinum surface covered by an electronically conducting monolayer of adsorbed oxygen (Pt–O). In addition, ellipsometry confirmed that the thickness of an adsorption layer does not exceed 10 Å, even in the Kolbe reaction region.<sup>8)</sup> Therefore, the incorporation of  $\text{CH}_3\text{COO}^-$  into the Pt–O layer seems more reasonably to be expected than that of the adsorption layer of  $\text{CH}_3\text{COO}^-$  onto the oxide film (PtO). Hence,  $C_{dl}$ , represented by  $C_H$ , is due to the specific adsorption of  $\text{CH}_3\text{COO}^-$  into the Helmholtz layer. This  $C_H$  can be explained on the basis of a Helmholtz parallel-plate condenser model:

$$C_{dl} \doteq C_H = \epsilon/4\pi d \quad (10)$$

where  $d$  is the distance between the condenser plates and  $\epsilon$  is the dielectric constant. Using a dielectric constant of acetic acid of 6.2 and a thickness of  $C_H$  of the order of 10 Å,  $C_H$  can be estimated to be about 6  $\mu\text{F}/\text{cm}^2$ . This  $C_H$  value is almost equal to those of  $C_{dl}$  and  $C_{HF}$  obtained from the Z plane plot and the  $Y/\omega$  plane plot respectively at 2.00 V.

The Kolbe reaction at the surface covered by  $\text{CH}_3\text{COO}^-$  or  $\text{CH}_3\text{COO}^\cdot$  at potentials above 2.00 V is due to:



**Gold Electrode.** The differential capacity on a gold anode in an aqueous acetate solution, as measured with an a.c. bridge in series with a capacitor and a resistor, increased markedly at potentials above 1.50 V.<sup>19)</sup>

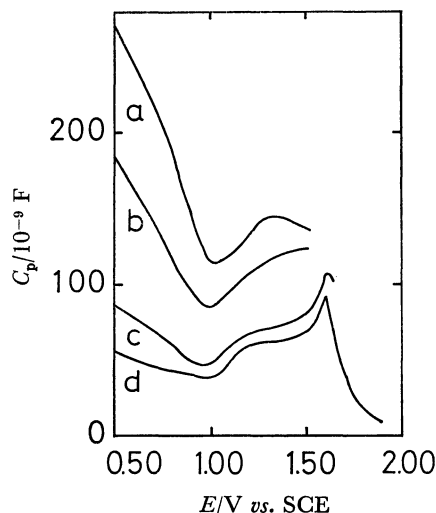


Fig. 6. Parallel capacitance vs. potential curves on Au in 2 M acetate with various frequencies. sweep rate: 10 mV/s, a: 20 Hz, b: 80 Hz, c: 400 Hz, d: 3 kHz.

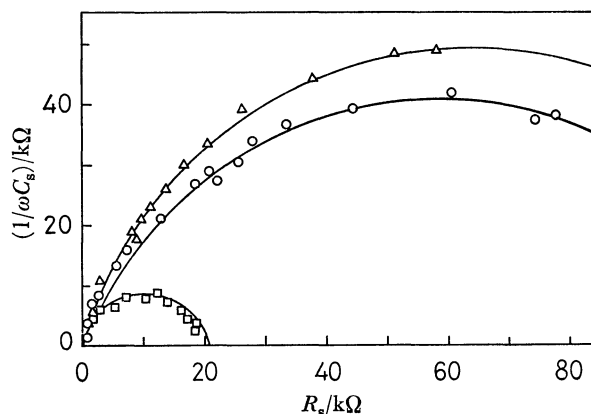
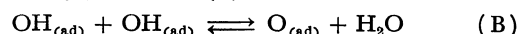
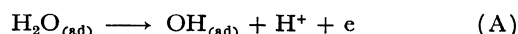


Fig. 7. Complex impedance plane plot of Au in 5 M acetate. -O-: 1.00 V, -Δ-: 1.30 V, -□-: 1.50 V.

Figure 6 shows the  $C_p$ – $E$  curves of gold anodes measured with the PSD in parallel with a capacitor and resistors. A constant value was reached at potentials above 1.60 V, in contrast to the results of a previous paper.<sup>19)</sup> In order to determine the rate-determining step of the oxygen evolution reaction in the presence of  $\text{CH}_3\text{COO}^-$  with gold anodes, the Z plane plot was worked out; the results are shown in Fig. 7. The rate-determining step that occurs at potentials above 1.36 V<sup>20)</sup> was found to be a charge-transfer process according to Eq. A, because the only semicircle was observed in the Z plane at 1.50 V.



The  $C_{dl}$  value on gold in a 5 M acetate solution is shown in Fig. 3.

The  $Y/\omega$  plane plot (Fig. 8) was worked out with a gold anode in an acetate solution in order to examine the behavior of  $\text{CH}_3\text{COO}^-$ , since the adsorption of  $\text{CH}_3\text{COO}^-$  on platinum occurs at around 1.30 V, with

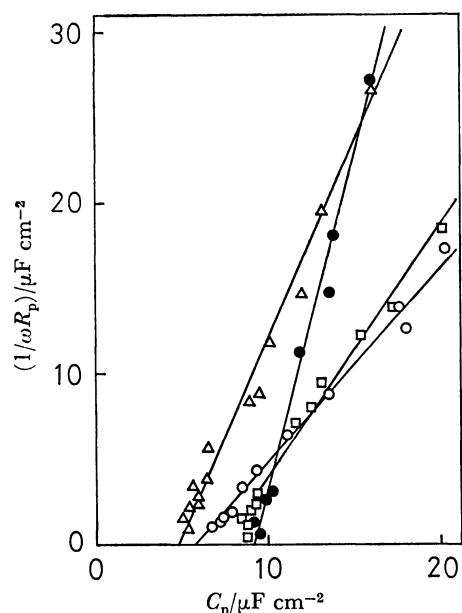


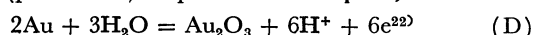
Fig. 8. Complex capacitance plane plot of Au in 2 M acetate.

—○—: 0.75 V, —△—: 1.00 V, —□—: 1.30 V, —●—: 1.50 V.

the evolution of oxygen. The loci of the plot in the potential range of 0.75 to 1.50 V differ from those on platinum anodes; they represent an approximately straight line without a specific circular arc. The  $C_{dl}$  value obtained at the intercept of the  $C_p$  axis (Eq. 6) is of the order of 6–10  $\mu\text{F}/\text{cm}^2$  in the potential range from 0.75 to 1.50 V. These potentials are on the  $Y/\omega$  plane. Since the presence of the semicircle or the quarter circle is quite doubtful, the adsorption of  $\text{CH}_3\text{COO}^-$  on a gold anode is unlikely. In addition, the surface coverage of  $\text{CH}_3\text{COO}^-$  on a gold anode is negligible at concentrations higher than 0.5 M, as has previously been reported.<sup>6)</sup>

Since the characteristics of the  $C_p$ – $E$  curve at potentials less than 1.50 V shown in Fig. 6 are similar to those of the capacity-potential curve of gold anodes in perchloric acid reported by Schmid and Hackerman,<sup>21)</sup> it may be concluded that the present  $C_p$ – $E$  curves are not affected by the adsorption of  $\text{CH}_3\text{COO}^-$ . According to Schmid and Hackerman,<sup>21)</sup> the capacity hump in the potential range from 0.9 to 1.3 V is due to the adsorption of oxygen-containing species, *i.e.*,  $\text{OH}^-$ ,  $\text{O}^{2-}$ , *etc.*

Thermodynamically, the formation of oxide on gold anodes at potentials above 0.93 V (*vs.* SCE) in acetate solutions (pH=4.80) is possible *via* Eq. D;



$$E^\circ = 1.457 - 0.591\text{pH} \text{ (vs. NHE)}$$

$E^\circ$ : equilibrium potential

Therefore, the adsorption of oxygen-containing species, *e.g.*, water, on gold seems reasonable.

The specific circular arc with gold anodes, however, was not observed on the  $Y/\omega$  plane at the potentials where the oxygen-containing species adsorbs. The quarter circle on platinum anodes was obtained on the  $Y/\omega$  plane in the potential range from 0.75 to 0.90 V,

where the first peak of the capacity was observed with the  $C_p$ – $E$  curves. In this potential range, the adsorption of oxygen-containing species on platinum anodes is possible.

The difference between the adsorption of oxygen-containing species on platinum and gold anodes is considered to be as follows. Since the adsorption of reacting species can be detected by the specific arc on the  $Y/\omega$  plane, the adsorption of oxygen-containing species on platinum is verified by the quarter circle. Water adsorbed on a gold anode is immediately changed to the oxide,  $\text{Au}_2\text{O}_3$ , according to Eq. D, and the surface is completely covered with the oxide.

Since the time constant of the adsorption layer differs from that of oxide, the  $Y/\omega$  plane plot with gold anodes will not show a circular arc indicating the adsorption.

The results presented above support the notion that the Kolbe reaction occurs on surfaces covered with  $\text{CH}_3\text{COO}^-$  or  $\text{CH}_3\text{COO}\cdot$ .<sup>3)</sup> The equivalent circuit of the oxygen evolution on a gold anode, which does not contain the adsorption pseudo-capacity of  $\text{CH}_3\text{COO}^-$ , is shown in Fig. 5b.

## References

- 1) T. Dickinson and W. F. K. Wynne-Jones, *Trans. Faraday Soc.*, **58**, 382, 388, 400 (1962).
- 2) K. Sugino, T. Sekine, and N. Sato, *Electrochem. Tech.*, **1**, 112 (1963).
- 3) A. K. Vijh and B. E. Conway, *Z. Anal. Chem.*, **224**, 160 (1967).
- 4) I. Sekine and T. Sekine, *J. Electrochem. Soc. Jpn.*, **36**, 201 (1968).
- 5) I. Sekine, *Denki Kagaku*, **40**, 156 (1972).
- 6) I. Sekine, *Denki Kagaku*, **41**, 412 (1973).
- 7) I. Sekine, *Denki Kagaku*, **43**, 313 (1975).
- 8) I. Sekine, K. Kudo, and G. Okamoto, *J. Res. Inst. Catal., Hokkaido Univ.*, **24**, 44 (1976).
- 9) A. Kunugi, S. Iseki, K. Ohashi, and S. Nagaura, *Denki Kagaku*, **37**, 41 (1969).
- 10) J. H. Sluyters, *Recl. Trav. Chim. Pays-Bas*, **79**, 1092 (1960).
- 11) K. Takahashi, *Electrochim. Acta*, **13**, 1609 (1968).
- 12) R. D. Armstrong, W. P. Race, and H. R. Thirsk, *J. Electroanal. Chem.*, **16**, 517 (1968).
- 13) M. Sluyters-Rehbach and J. H. Sluyters, "Electroanalytical Chemistry," ed. by A. J. Bard, Marcel Dekker, Inc., New York (1970), Vol. 4, p. 1.
- 14) A. P. Tomilov, S. G. Mairanovskii, M. Ya. Fioshin, and V. A. Smirnov, "The Electrochemistry of Organic Compounds," Halsted Press, New York (1972), p. 379.
- 15) R. Payne, "Techniques of Electrochemistry," ed. by E. Yeager and A. J. Salkind, Wiley-Interscience, New York (1972), Vol. 1, p. 120.
- 16) R. DE Levie, *Electrochim. Acta*, **10**, 395 (1965).
- 17) J. P. Hoare, "The Electrochemistry of Oxygen," Interscience, New York (1968), p. 84.
- 18) B. E. Conway and A. K. Vijh, *Chem. Rev.*, **67**, 623 (1967).
- 19) I. Sekine and T. Sekine, *Denki Kagaku*, **36**, 286 (1968).
- 20) See also p. 87 in Ref. 17.
- 21) G. M. Schmid and N. Hackerman, *J. Electrochem. Soc.*, **109**, 243 (1962).
- 22) M. Pourbaix, "Atlas of Electrochemical Equilibria in Aqueous Solutions," Pergamon Press, Cebelcor (1966), p. 399.